Igor Solodov[1]*, Damien Ségur[2] and Marc Kreutzbruck[1]
[1]*Institut für Kunststofftechnik, Universität Stuttgart, Stuttgart, Germany*
[2]*CEA LIST, CEA Saclay, 91191 Gif-sur-Yvette, France*

Recognition of bonding contamination in CFRP composite laminates by measurements of local vibration nonlinearity

Identyfikacja zanieczyszczeń w połączeniach klejonych kompozytów CFRP poprzez pomiary lokalnej nieliniowości drgań

ABSTRACT

A new approach based on measurements of a local nonlinear response of the laminate is suggested and applied to characterizing contaminations of adhesive bonding in carbon fibre reinforced polymer (CFRP). It is shown that a contaminated boundary layer of the adhesive contributes to an overall nonlinear response of the laminate that enables to recognise the difference in bonding quality caused by various types and levels of contaminations.

Keywords: *glue bond; CFRP composite; vibration measurement*

STRESZCZENIE

W artykule, w celu scharakteryzowania zanieczyszczeń połączeń klejonych polimerów wzmocnionych włóknem węglowym (CFRP), zaproponowano i następnie zastosowano nowe podejście oparte na pomiarach lokalnej nieliniowej odpowiedzi laminatu. Pokazano, że zanieczyszczona warstwa graniczna kleju przyczynia się do ogólnej nieliniowej odpowiedzi laminatu, która umożliwia rozpoznanie różnicy w jakości wiązania spowodowanej różnymi typami i poziomami zanieczyszczeń.

Słowa kluczowe: *połączenie klejowe; kompozyt CFRP; pomiar drgań*

1. Introduction

Adhesively bonded composite parts are increasing alternatives to mechanical joints in engineering applications of composite materials. The need for adequate nondestructive evaluation (NDE) and characterization of interfacial adhesion which determines reliability of structural bonding has long been considered as a challenge for ultrasonic NDE [1].

Conventional ultrasonic NDE instruments used in industry and technology make use of the so-called linear elastic response of materials which results in the amplitude and phase variations of the input signal due to its interaction with defects. The nonlinear approach to ultrasonic testing is concerned with nonlinear material response related to the frequency changes of the input signal. These spectral changes are caused by nonlinear dynamics of solids which scales from inter-atomic level for perfect materials to meso- and macro-scale nonlinearity for damaged areas. In many cases, monitoring material nonlinearity reveals directly the vulnerable areas within material or a product with sensitivity far superior to traditional ultrasonic inspection [2].

The nonlinear approach to material characterization stems from classical nonlinear acoustics [3, 4] which studied quasi-perfect (crystalline) materials whose nonlinearity was concerned with weak nonlinear dynamics of inter-atomic (Van der Waals) forces and described by generalised Hooke`s law:

$$\sigma(\varepsilon) = C^{II}(1 - \beta_2\varepsilon - \beta_3\varepsilon^2 + ...)\varepsilon \qquad (1)$$

where C^{II} is a linear material stiffness, β_n are nonlinear moduli of various orders.

The manifestation of elastic nonlinearity in (1) is the generation of the higher harmonics (frequencies nf_0) in the propagating high-amplitude ultrasonic wave of the fundamental frequency f_0. Normally, the most sufficient contribution to the higher harmonic package comes from the second harmonic which is mainly used in applications and whose normalised amplitude is a parameter to characterise material nonlinearity.

From (1), the ratio of the second harmonic to the fundamental frequency signal is $\sim\beta_2\varepsilon$. For all "classical" (flawless) materials $\beta_2 \sim 1 \div 10$, so that even for a high acoustic strain values ($\varepsilon \approx 10^{-4}$) the above ratio $\leq 10^{-3}$. As the nonlinear wave propagates, the higher harmonic contribution leads to the waveform distortion which accumulates with propagation distance. This benefit is used to enhance the second harmonic response at the detector position. However, in reality even for a high acoustic strain of fundamental frequency the normalised cumulative second harmonic amplitude in majority of "classical" materials is substantially < 1%.

In general, a non-perfect structure of realistic materials provides higher material nonlinearity attributed to different new mechanisms of acoustic nonlinearity. A substantial enhancement of the second harmonic signal was measured in a high-purity Al single crystal in which a dislocation pattern was induced by mechanical stress applied [4]. Further investigations confirmed an important role of internal boundaries in nonlinearity enhancement for dislocations in fatigued materials [5] and matrix-precipitate interfaces in alloys [6].

*Correspondence author. E-mail: igor.solodov@ikt.uni-stuttgart.de

DOI: 10.26357/BNiD.2018.001

Numerous studies were implemented to identify the mechanisms and manifestations of the nonlinearity for imperfect interfaces in application to NDE of closed cracks. It was found that various nonlinear mechanisms, which include plasticity of asperities [7], hysteretic nonlinearity [8], etc. provide a substantial enhancement of the interface nonlinear response. A further increase of Contact Acoustic Nonlinearity (CAN) was revealed for "weaker" bonds with intermittent contact ("clapping") induced by an acoustic wave [9, 10].

Much less attention has been paid to nonlinearity of adhesively bonded interfaces. In this case, the joining materials are connected by means of an adhesive layer which forms two perfect interfaces between the materials and adhesive. The joint can now be represented as a nonlinear spring with a stress-strain response dependent on elastic properties of the adhesive itself as well as thin boundary layers (~ μm size) between the adhesive and the adherends [11]. The calculations revealed [11] that both linear and nonlinear parameters of these layers impact strongly the S-shaped classical stress-strain curve (1) of the joint and thus modify its nonlinear response. Further calculations [12] proposed to use the higher harmonics of slanted longitudinal waves reflected from the interface for NDE of adhesive joints.

The bulk wave reflection geometry is not applicable for composite materials manufactured mainly in the form of plates. A direct way to evaluate elastic nonlinearity in composite laminate plates is based on the second harmonic measurements for propagating Lamb modes. This technique is believed to be prospective for plate-like metallic and composite specimens and received considerable attention in literature e.g. [13-15].

To generate the so-called cumulative second harmonic of a Lamb wave mode, however, the two crucial conditions are required to be satisfied: phase velocities of the fundamental and the second harmonic modes must be equal and the power flow between them must be non-zero. Due to Lamb wave dispersion, the first condition leads a strict selection of the frequencies and the types of modes which are to be phase matched. For a uni-directional CFRP plate, the selection of these parameters identifies modes S_1 and S_2 as possible candidates for cumulative second harmonic generation [14]. In addition, the fundamental frequency f_0 must be chosen from the relation: $f_0 D \approx 2.25$ (MHz). These conditions have been recently confirmed and generalised for the case of a symmetric ply structure in CFRP laminate $[\pm 45/0/90]_{Sym}$ [15]: In addition to S_1-S_2 pair another three possible pairs S_2-S_2, S_3-S_3, and S_7-S_{12} have been obtained with different relations for selection of the fundamental frequency $f_0 D \approx 0.5$ (MHz · mm) for the first two pairs and $f_0 D \approx 2.234$ (MHz · mm) for S_7-S_{12} interaction (Fig. 1 [15]). The highest efficiency of the second harmonic generation is predicted for the last pair due to precise phase velocity match.

The strict conditions for selection of the experimental parameters make the nonlinear plate wave technique barely applicable in industrial environment (various lay-ups, thickness, curved specimens, etc.). Instead, a new approach proposed in this paper makes use of a local nonlinear response of the plate deformation. A contaminated layer of the adhesive is supposed to have a contribution to an overall nonlinear response of the laminate that enables to recognise the difference in bonding quality.

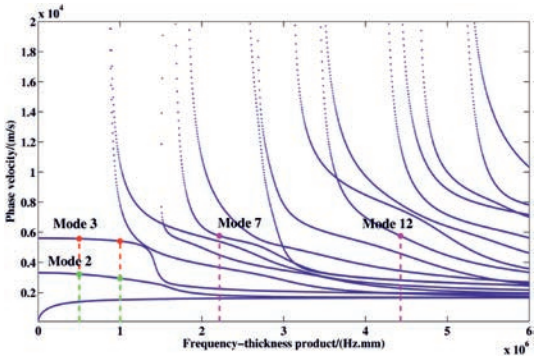

Fig. 1. Mode selection for second harmonic generation in symmetric CFRP laminate $[\pm 45/0/90]_{Sym}$ [15]
Rys. 1. Wybór trybu generowania drugiej harmonicznej w symetrycznym laminacie CFRP $[\pm 45/0/90]_{Sym}$ [15]

2. Local generation of non-cumulative higher harmonics

Cumulative nonlinear generation for the plate modes uses the benefit of the second harmonic growth with propagation distance that enables to increase its amplitude at the detector position. This approach originated and was inevitable in classical nonlinear acoustics which studied perfect (crystalline) materials whose nonlinearity was concerned with weak nonlinear dynamics of inter-atomic forces. In materials with internal boundaries, the nonlinearity is noticeably higher so that the nonlinear measurements can be implemented locally without higher harmonic accumulation with distance.

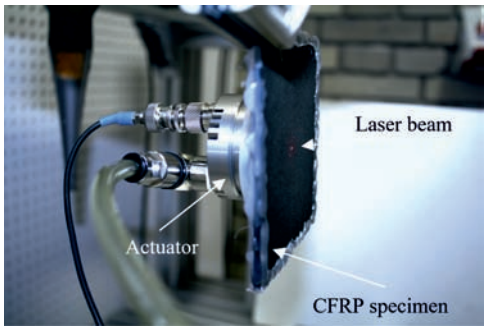

Fig. 2. Excitation and detection of vibrations in CFRP specimen
Rys. 2. Wzbudzenie i detekcja drgań w próbce CFRP

The technique is therefore based on the local generation of high amplitude vibrations and detecting the higher harmonics in the excitation area. An option for higher amplitude excitation was found by using piezo-actuators manufactured by SI Scientific Instruments GmbH (Germany) with a frequency response extended from low kHz into high kHz range (above 100 kHz). The actuators are vacuum attached to the specimens and can be used for on-site measurements of large aviation components. They are driven by a CW voltage generated by the HP 33120A arbitrary waveform generator. The generator is combined with HVA-B100 amplifier to

result in 10 ÷ 40 V input amplitude for the piezo-actuator. The actuator is attached to one of the sides of the specimen and nonlinear vibrations produced locally in the area of excitation are measured on the opposite side of the specimen (Fig. 2).

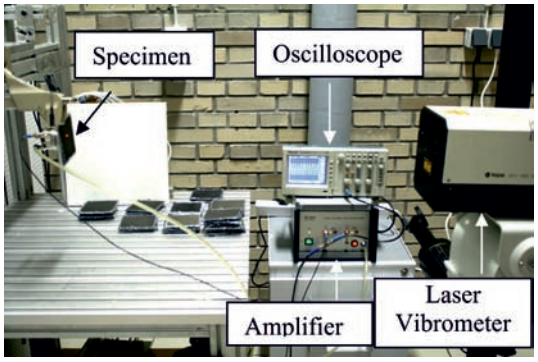

Fig. 3. Experimental setup used for excitation/detection of vibrations in CFRP specimen
Rys. 3. Układ eksperymentalny stosowany do wzbudzania/wykrywania drgań w próbce CFRP

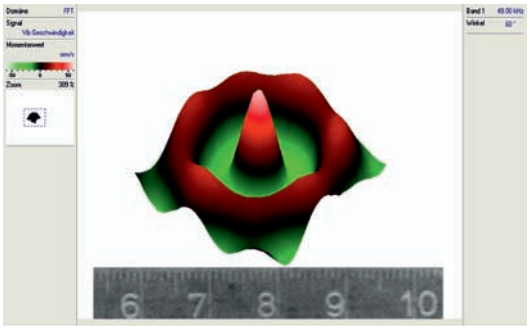

Fig. 4. Vibration pattern in the excitation area
Rys. 4. Wzorzec wibracji w strefie wzbudzenia

To receive and analyze the frequency content of the vibrations generated locally in the excitation area a scanning laser vibrometer (SLV, Polytec 300) operating in the vibration velocity mode with maximum frequency bandwidth of 1.5 MHz was used (Fig. 3). The dynamic range of the SLV measurements (100 ÷ 120 dB) is well beyond the level of nonlinear frequency components. To avoid an impact of reflections on the local vibration in the excitation area, the edges of specimens were covered with dissipative material and rather high vibration frequency was chosen (49 kHz). With these precautions, after scanning of the specimen surface, the image of the fundamental frequency vibration pattern in the specimen is obtained as the wave emanating from the excitation area. The spectrum and the temporal pattern of the vibrations are measured in the central (source) area (a circle with 5 mm radius) where no plate wave propagation is involved yet (Fig. 4).

For input voltage of 20V, the vibration velocity amplitude measured at 49 kHz was in the range of 130-150 mm/s. The displacement amplitude is therefore in the range of (4-5)10-8 m so that a local strain developed in the excitation area is 10-5. This deformation is sufficient for manifestation of noticeable local nonlinearity in composite materials.

3. Verification of the methodology

To verify the methodology a few tests were implemented with knowingly nonlinear contacts in delaminated areas in CFRP specimens. A part of one of such specimens is shown in Fig. 5: the delamination between a few surface plies in a large CFRP plate (300x300x4 mm3) was induced by local surface heating. The local spectra obtained for the transducer positions inside the delamination area (on the reverse side of the plate) and outside (2 cm apart) are shown in Fig. 6. As expected, a certain level of nonlinearity is detected in the intact composite area (Fig. 6, top). A substantial increase of the number and the amplitudes of the higher harmonics in the damaged area due to CAN is clearly seen (Fig. 6, bottom) that confirms workability of the technique which was also tested on various other defects in CFRP.

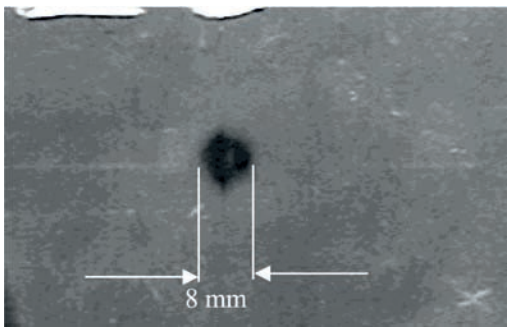

Fig. 5. A heat damaged area in a CFRP plate used for testing the local nonlinear methodology
Rys. 5. Obszar uszkodzenia cieplnego na płycie CFRP wykorzystywany do testowania lokalnej nieliniowej metodologii

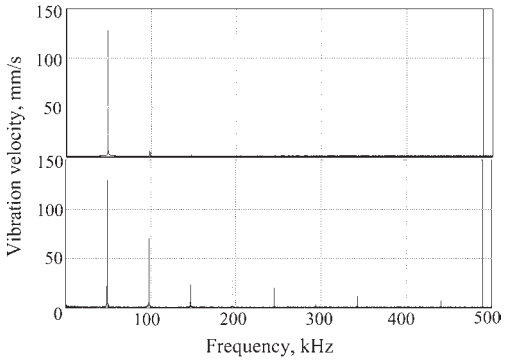

Fig. 6. Vibration spectra outside (top) and inside the damaged area (bottom) for CFRP specimen shown in Fig. 5.
Rys. 6. Widma drgań na zewnątrz (u góry) i wewnątrz uszkodzonego obszaru (u dołu) dla próbki CFRP pokazanej na Rys. 5.

4. Description and testing of contaminated specimens

4.1 Sample preparation

The measurements were carried out for a large set of composite specimens with different bonding conditions. The samples (10 x 10 cm^2) manufactured according to Airbus AIPS 03-02-019 comprised two 8-ply CFRP laminates bonded with an epoxy adhesive layer FM300K from Cytec®. Hexcel M21E® is the material that was used for the composite laminates with the given stacking sequence [0, 0, 45, -45, -45, 45, 0, 0].

Two typical stages during the life of a structural part for which the adhesive properties of a bonding joint could be degraded were considered: the production process and the maintenance and repair scenario. All samples for production scenarios were bonded by using the adhesive FM® 300K (0.2) from Cytec while the specimens for repair scenarios were bonded by using the adhesive FM® 300-2.

For production scenario, three kinds of contaminants were studied: Release agent (RA), fingerprint (FP) and moisture (MO).

Release agent (silicon-based) is used during the molding process to ease the demolding of the parts. The release agent used was FREKOTE® 700NC. It was applied to the surfaces by dip coating before bonding.

Moisture uptake is relevant to both manufacturing and repair scenarios due to possible penetration of moisture during nondestructive testing, wet abrasion or storage in humid atmosphere. Moisture samples to be bonded were dried in an oven at 80°C until mass constancy. Then they were stored in a climate chamber (70°C, defined relative humidity) for two weeks prior to bonding to a reference bonding partner. The following relative humidity conditions were adjusted in the chamber: MO1: 30%; MO2: 75% and MO3: 98% relative humidity.

Fingerprint is typical for both manufacturing and repair scenarios due to inappropriate handing of the part. Samples were prepared using a standardized salty fingerprint solution (artificial hand perspiration solution) according to DIN ISO 9022-12. This solution contains sodium chloride, urea, ammonium chloride, lactic acid, acetic acid, pyruvic acid and butyric acid in demineralized water. Samples were prepared by applying this solution with the size of a fingerprint to the samples. Various degrees of contamination were achieved by using different dilutions (with demineralized water) of the FP solution: FP1: 10% FP solution, FP2: 50% FP solution and FP3: pure FP solution.

For repair scenario, only one kind of contaminant was applied: De-icing fluid (DI). The other two processes that could result in a loss of adhesion due to external influences or errors during bonding process were also studied: Thermal degradation (TD) and Faulty Curing (FC).

De-icing fluid is relevant to the repair environment: Residues of potassium formiate of the de-icing fluid on the outer surface of an aircraft may end up in the repair areas and finally lead to an adhesive failure of the bonding. The de-icer used was SAFEWAY®KF from CLARIANT. It was diluted with demineralized water to obtain solutions with the following concentrations in percent of volume: 2% (DI1), 7% (DI2), and 10 % (DI3). The solution was applied to the surfaces by dip coating (aqueous solution) and dried in the oven for 2h at 40°C.

Thermal degradation can cause local overheating and damage of resin in CFRP. For different degrees of thermal degradation the samples were stored for 2h at the following elevated temperatures: 220°C (TD1), 260°C (TD2), and 280°C (TD3).

Faulty Curing: Inappropriate use of the adhesive or wrong curing cycles may lead to a loss of the adhesive properties in both manufacturing and repair scenarios. An IR spot light was used to perform the adhesive curing, and the temperatures used were as follows: 120°C (FC1), 140°C (FC2), and 160°C (FC3).

For each type of contamination in both scenarios, a set of three specimens of every level of contamination was prepared for reliable statistics. Along with other three reference specimens (REFR and REFP) for each of the scenarios a total number of the specimens to be tested amounted to 60.

4.2 Testing of contaminated specimens

A characteristic spectrum measured in the contaminated specimens usually contained 2-3 higher harmonics with minor but noticeable waveform distortion (Fig. 7) which is typical for the materials without severe damage (delaminations or obvious disbonds) in composites.

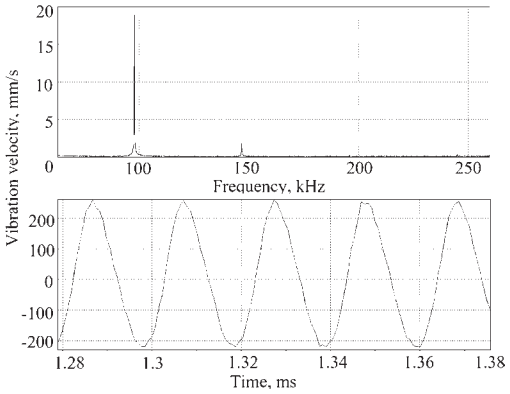

Fig. 7. A typical higher harmonic part of the vibration spectrum (second and third harmonics top) and vibration pattern (bottom) in contaminated CFRP specimen FP2-3

Rys. 7. Typowa część widma drgań wyższych harmonicznych (górna i trzecia harmoniczna) i wzorzec wibracji (dół) w zanieczyszczonej próbce CFRP FP2-3

One of the experimental problems found out was concerned with an intermittent contact between the tip of vacuum attached transducer and the specimen that resulted in unstable vibrations and spectra in some points over the measurements area. To overcome the problem the spectra and the vibration temporal patterns were monitored for each scanning point around the excitation area. The measurements were counted as valid only when they demonstrated stable spectra in time. Each value of the fundamental frequency vibration velocity (v_0) and the higher harmonic components (v_n) measured for a stable spectrum in the probing area was used for evaluation of the nonlinear ratio $N_i = \sum v_n^2 / v_0^2$. An average value of the nonlinear ratio in the probing area was then calculated $N = \sum_{i=1}^{m} N_i / m$ (where m is the number of measurements) and the standard deviation of the results was estimated as

$$\Delta N = \sqrt{\sum_{i=1}^{m} (N_i - N)^2 / m(m-1)}$$

The measurements were repeated in various points over the central part of the specimen to provide the relative error $\Delta N/N \leq 10 \div 20\%$.

The nonlinear ratio N_i is a part of the vibration energy ($\sim v_0^2$) converted into the higher harmonics ($\sim v_n^2$) so that it clearly quantifies material nonlinearity. An alternative parameter used in the literature is the nonlinearity parameter β_2 (see (1)) which is proportional to the second harmonic amplitude normalised to the square of the fundamental frequency wave. This ratio is an amplitude-independent parameter in "classical" (homogeneous flawless) materials with power-law dependence of the higher harmonic amplitudes (quadratic for the second harmonic). This is not the case in composites where the diverse nonlinear mechanisms change the power-law dynamics and selection of the amplitude-independent parameter is barely possible. To avoid the influence of the amplitude-dependent effects in estimation of the nonlinear ratio N the amplitude of the input voltage of the transducer was kept constant (20 V) over the course of measurements. As a result, in all the specimens measured the fundamental vibration amplitude was virtually constant within ~10% deviation.

5. Experimental results

The results of the measurements and calculations of for all specimens (30 repair scenario (9TD, 9DI, 9FC, 3 REFR) and 30 production scenario (9MO, 9RA, 9FR, 3 REFP)) are given in Figs. 8-15. For each type of contamination, the data is structured in three sets of the specimens with the same specimen index (-1, -2, -3) but with a different level of contamination (numbers 1, 2, 3). The level of contamination enhances as this number increases. For the reference specimens, which are free from any contamination, the average values of (AV) are also calculated (Fig. 8 and Fig. 9).

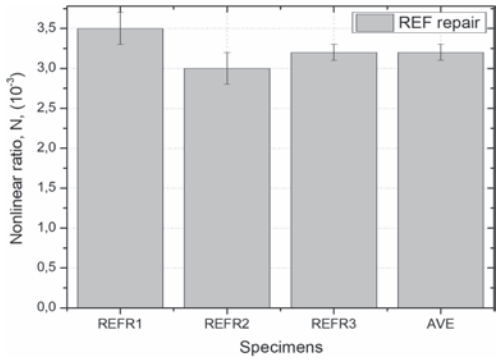

Fig. 8. Nonlinear ratios for reference specimens of repair scenario

Rys. 8. Współczynniki nieliniowe dla wzorców referencyjnych scenariusza naprawy

According to Fig. 8 and Fig. 9, the reference specimens reveal the minimal values of 3. The insertion of adhesive noticeably enhances the nonlinearity for all specimens by 1.5 - 2 times. The maximum nonlinear ratio was obtained in TD 3-2 specimen (, outside the scale in Fig. 10). In this specimen, the values were found to depend on the position of the measurement point. This fact, along with anomalously high value of the nonlinear ratio indicates the presence of local delamination in the specimen induced by thermal activation that has also been verified with conventional (linear) ultrasonics [16].

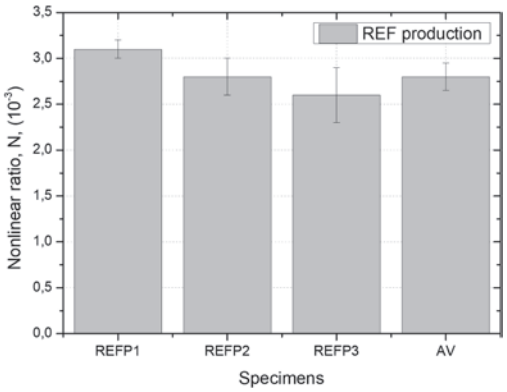

Fig. 9. Nonlinear ratios for reference specimens of production scenario

Rys. 9. Współczynniki nieliniowe dla referencyjnych próbek scenariusza produkcji

For each type of contamination, the values of change noticeably with variation of the contamination level that indicates the sensitivity to the changes in the contaminated boundary layer between the adhesive and the adherends. According to the measurement results, the sensitivity of the nonlinear method is, therefore, sufficient to recognize the effect of contamination on the adhesive bonding.

For the contaminations types TD, RA, FP, DI, and FC, material nonlinearity increases with the increase of the level of contamination (Fig. 10 – Fig. 14).

To correlate particular variations in with the strength of bonding as a function of the level of contamination we turn to the Introduction section where numerous examples were given to relate the increase in nonlinearity to "softening" of the material due to fatigue, cracking, internal interfaces, etc. A similar conclusion can be drawn based on the calculations of the stress-strain relations for the adhesive layer [11] which show that "softening" of the boundary layer increases its nonlinear response. This also correlates with a general characteristic of acoustic nonlinearity that is related to the material thermal expansion which is negligible for stiff materials and enhances strongly in soft solids [17].

This fact explains the lowest values of the nonlinear ratios in the reference specimens: Being free from any contamination they are supposed to manifest the highest bonding strength. From this viewpoint, the strongest decrease in bonding strength is caused by level 3 TD contamination (N values from ~8 to ~50, Fig. 10). A similar decrease in bonding strength is also recognized for level 3 DI, FP, RA, and FC contaminations (N values > 7, Fig. 11 – Fig. 14).). The MO case is not so convincing: with exception of the abrupt kick for specimen MO1-1, the nonlinearity does not change noticeably so that N oscillates around the value of 5 for all 3 levels of contamination.

6. Summary and conclusions

A new approach to characterizing contaminations of adhesive bonding is based on measurements of a local nonlinear response of the laminate. It is shown that a contaminated boundary layer of the adhesive contributes to an overall nonlinear response of the laminate that enables to recognise the difference in bonding quality caused by various types

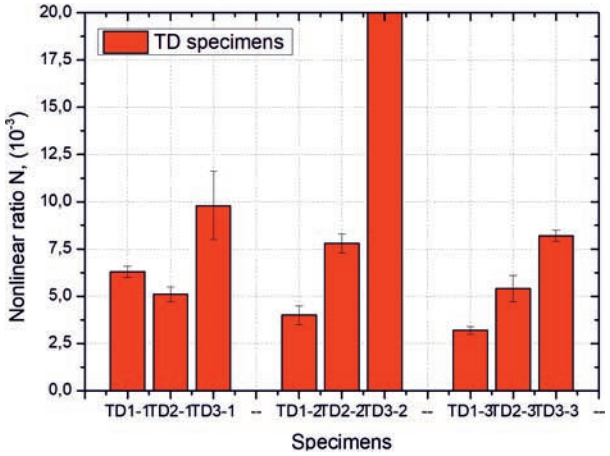

Fig. 10. Nonlinearity of the contaminated specimens (-1, -2, -3) as a function of TD level of contamination
Rys. 10. Nieliniowość zanieczyszczonych próbek (-1, -2, -3) w zależności od poziomu TD zanieczyszczenia

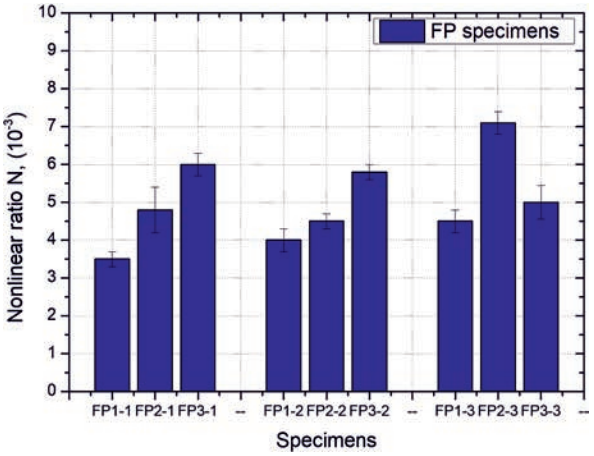

Fig. 13. Nonlinearity of the contaminated specimens (-1, -2, -3) as a function of FP level of contamination
Rys. 13. Nieliniowość zanieczyszczonych próbek (-1, -2, -3) w zależności od poziomu FP zanieczyszczenia

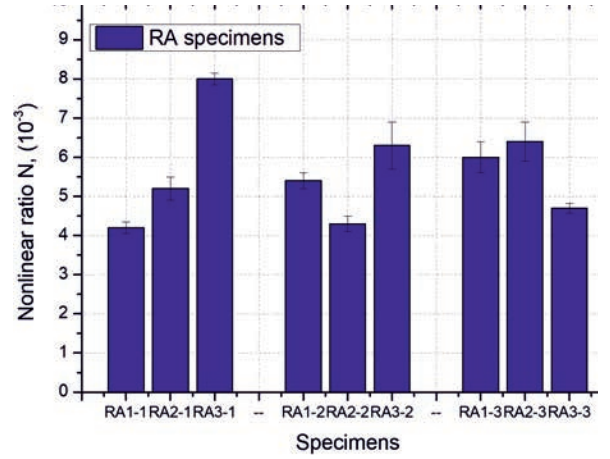

Fig. 11. Nonlinearity of the contaminated specimens (-1, -2, -3) as a function of RA level of contamination
Rys. 11. Nieliniowość zanieczyszczonych próbek (-1, -2, -3) w zależności od poziomu RA zanieczyszczenia

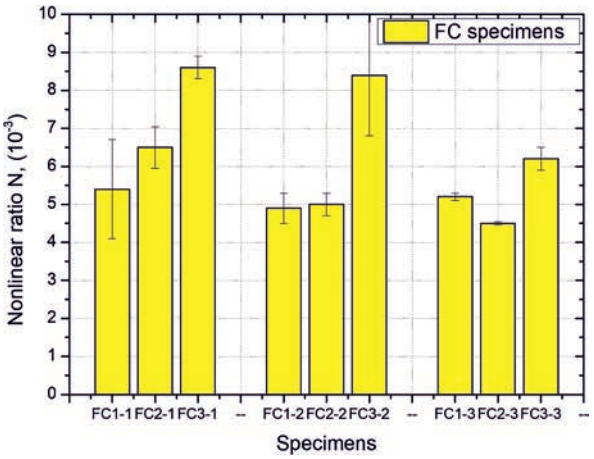

Fig. 14. Nonlinearity of the contaminated specimens (-1, -2, -3) as a function of FC level of contamination
Rys. 14. Nieliniowość zanieczyszczonych próbek (-1, -2, -3) w zależności od poziomu FC zanieczyszczenia

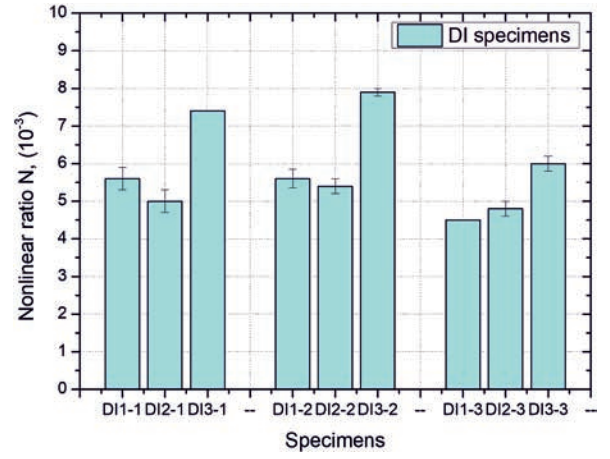

Fig. 12. Nonlinearity of the contaminated specimens (-1, -2, -3) as a function of DI level of contamination.
Rys. 12. Nieliniowość zanieczyszczonych próbek (-1, -2, -3) w zależności od poziomu DI zanieczyszczenia

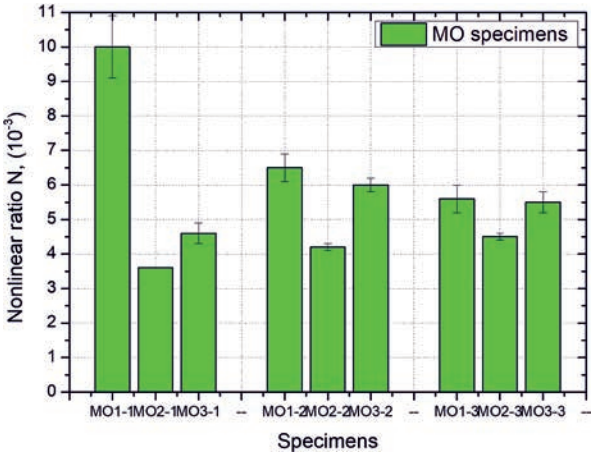

Fig. 15. Nonlinearity of the contaminated specimens (-1, -2, -3) as a function of MO level of contamination
Rys. 15. Nieliniowość zanieczyszczonych próbek (-1, -2, -3) w zależności od poziomu MO zanieczyszczenia

and levels of contamination.

According to the measurement results, all kinds of the contaminations studied in the context of aviation applications result in enhancement of the nonlinear response of the CFRP laminate which is an indication of deterioration of bonding quality. An anomalous increase in nonlinearity is revealed for a high level of thermal degradation that illustrates a strong loss of bonding strength induced by thermal degradation. A similar (but somewhat lower) increase in nonlinearity reveals and quantifies decrease in bonding strength caused by finger prints and release agent (composite component production scenario), di-icing fluid and faulty curing (repair scenario) contaminations.

7. Acknowledgement

This research is supported by European Union's Horizon 2020 research and innovation programme under grant agreement No 636494, project ComBoNDT (Quality assurance concepts for adhesive bonding of aircraft composite structures by advanced NDT).

8. References/Literatura

[1] H. N. G. Wadley, "Interfaces: The next NDE challenge", in Review of Progress in Quantitative Nondestructive Evaluation. Boston, MA: Springer US, pp. 881–892, 1988. DOI 10.1007/978-1-4613-0979-6_1

[2] P. Nagy, "Fatigue damage assessment by nonlinear ultrasonic material characterization", Ultrasonics, vol. 36, no. 1-5, pp. 375-381, 1998. DOI 10.1016/s0041-624x(97)00040-1

[3] M. A. Breazeale, J. Philip, "Determination of third-order elastic constants from higher harmonic generation", Physical Acoustics, vol. 17, New York, Academic Press, 1965.

[4] A. Gedroitz, V. A. Krasilnikov, "Elastic waves of finite amplitude and deviations from Hooke`s law", Soviet Physics JETP, vol. 16, pp. 1122-1131, 1963.

[5] W. T. Yost, J. Cantrell, "Materials characterization using acoustic nonlinearity parameters and harmonic generation: Engineering materials", in Review of Progress in Quantitative Nondestructive Evaluation, vol. 9, Springer, Boston, MA, pp. 1669–1676, 1990. DOI 10.1007/978-1-4684-5772-8_215

[6] J. Cantrell, W.T. Yost, "Effect of precipitate coherency strains on acoustic harmonic generation", Journal of Applied Physics, vol. 81, no. 7, pp. 2957-2962, 1997. DOI 10.1063/1.364327

[7] J. Kim, A. Baltazar, J. W. Hu, S. I. Rokhlin, "Hysteretic linear and nonlinear acoustic responses from pressed interfaces", International Journal of Solids and Structures, vol. 43, no. 21, pp. 6436-6452, 2006. DOI 10.1016/j.ijsolstr.2005.11.006

[8] P. Johnson, R. Guyer, Nonlinear mesoscopic elasticity. Weinheim: Wiley-VCH, 2009.

[9] I. Solodov, "Ultrasonics of nonlinear contacts: Propagation, reflection and NDE-applications", Ultrasonics, vol. 36, no. 1-5, pp. 383-390, 1998. DOI 10.1016/s0041-624x(97)00041-3

[10] I. Solodov, N. Krohn, G. Busse, "CAN: An example of nonclassical nonlinearity in solids", Ultrasonics, vol. 40, no. 1-8, pp. 621-625, 2002. DOI 10.1016/s0041-624x(02)00186-5

[11] J. D. Achenbach, O. K. Parikh, "Ultrasonic detection of nonlinear mechanical behaviour of adhesive bonds", in Review of Progress in Quantitative Nondestructive Evaluation, vol. l0 B, Springer, Boston, MA, pp. 1837-1844, 1991. DOI 10.1007/978-1-4615-3742-7_91

[12] Z. An, X. Wang, M. Deng, J. Mao, M. Li, "A nonlinear spring model for an interface between two solids", Wave Motion, vol. 50, no. 2, pp. 295–309, 2013. DOI 10.1016/j.wavemoti.2012.09.004

[13] L.J. Jacobs, J. Kim, J. Qu, "Characterization of fatigue damage in nickel-base superalloy using nonlinear ultrasonic waves", in Proc. Int. Congress on Ultrasonics, Vienna, 2007.

[14] W. Li, Y. Cho, J. D. Achenbach, "Detection of thermal fatigue in composites by second harmonic Lamb waves", Smart Materials and Structures, vol. 21, no.8, p. 085019, 2012. DOI 10.1088/0964-1726/21/8/085019

[15] J. Zhao, V. K. Chillara, B. Ren, H. Cho, J. Qiu, and C. J. Lissenden, "Second harmonic generation in composites: Theoretical and numerical analyses", Journal of Applied Physics, vol. 119, no. 6, p. 064902, 2016. DOI 10.1063/1.4941390

[16] P. Malinowski, R. Ecauilt, T. Wandowski, W. Ostachowicz, "Evaluation of adhesively bonded composites by nondestructive technique", in Proceedings of the SPIE Smart Structures/NDE, Health Monitoring of Structural and Biological Systems 2017, 2017. DOI 10.1117/12.2259852

[17] Y. Zheng, R. Maev, I. Solodov, "Nonlinear acoustic applications for material characterisation: A review", Canadian Journal of Physics, vol. 77, pp. 927-967, 1999. DOI 10.1139/p99-059